Swept-Volume-Aware Planning and Control for Multi-Axle Swerve-Drive AMRs

Tianxin Hu[1], Shenghai Yuan[1*], *Member, IEEE*,
Zeqing Zhang

***Abstract*—We present a framework for multi-axle swerve-drive AMRs that jointly addresses swept-volume-aware planning and trajectory tracking. The planner combines MINCO trajectory optimization with Signed Distance Field (SDF) obstacle costs and a swept-area penalty, generating smooth and safe trajectories in constrained spaces. The tracker uses model predictive control (MPC) on a point-mass model and maps the optimal control vector to wheel-group steering angles and speeds for full independent steering. In simulation with a 5-axle vehicle, the proposed method reduces excess swept area and maintains accurate tracking while meeting real-time requirements. The approach is practical for logistics scenarios where large vehicles operate near obstacles and pedestrians.**

***Index Terms*—LIDAR, Multi-Axle, AMRs, SDF, Trajectory Estimation.**

I. Introduction

Logistics is a vital component of modern society, which facilitates the flow of goods and services. Although large multi-axle trucks [1], [2] offer capacity and efficiency, they face several significant maneuverability challenges [3] in constrained urban environments.

A critical challenges is the swept volume [4], [5] of multi-axle vehicles, as the rear axles follow different paths from the front during turns [6], as shown in Fig. 1. This increases the risk of entering adjacent lanes, sidewalks, or obstacles. Current automated driving systems are insufficient for addressing this problem, as they are primarily designed for smaller vehicles [7] (i.e., cars) and fail to optimize for the unique dynamics of multi-axle configurations [1].

The challenge lies in managing the swept volume while ensuring that each axle follows a safe and efficient path in real-time [4], [5]. Existing methods for path planning [8]–[19] and control [20]–[29] typically simplify the vehicle as a single rigid body [30], which does not account for the independent control needed for each axle in multi-axle systems. As a result, these approaches [8]–[29] struggle to minimize swept volume, especially in complex environments.

To address this challenge, we propose a novel approach that integrates swept volume-aware path planning with model predictive control (MPC) for Swerve-Drive autonomous mobile robots (AMR) systems. Our method optimizes the trajectory of the vehicle in real-time, minimizing the swept volume while allowing each wheel to turn independently. By utilizing MPC, we can predict the future state of the vehicle and adjust the turning radius of each wheel, ensuring precise navigation through tight spaces without compromising safety or efficiency. This approach not only tackles the limitations of current systems, but also sets the foundation for safer and more robust multi-axle AMR operations in real-world environments. By reducing swept volume and improving control over each axle, our method paves the way for more reliable autonomous heavy vehicles, particularly in logistics and industrial applications.

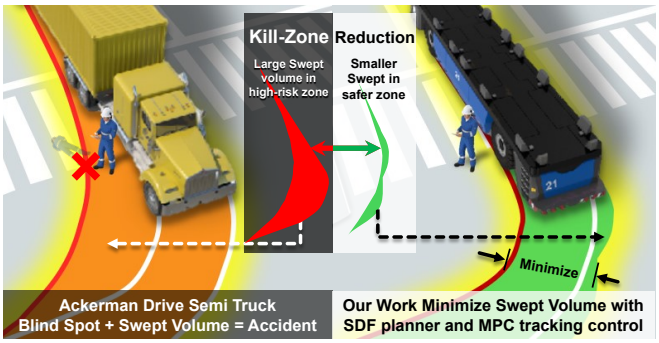

Fig. 1: This work aims to reduce the minimal swept volume and ensure stable trajectory tracking, enhancing safety in industrial applications.

The main contributions of this work are as follows.

- We propose a unified approach that integrates swept volume-aware path planning with MPC to optimize the trajectory and independently control each wheel of multi-axle AMRs, ensuring precise maneuverability in constrained environments.
- We propose a method for calculating the steering angles of each wheel group in multi-axle vehicles based on velocity vectors, simplifying the vehicle model and facilitating the use of MPC control.
- We validate the approach, showing significant reductions in swept volume and improved real-time trajectory tracking using CUDA, enabling more reliable and efficient autonomous heavy-duty AMR applications.
- We will open-source our work for the benefit of the community. https://github.com/ccwss-maker/svplan

II. Related Work

Prior studies either focus on swept-volume-aware planning [4], [5], [31] or on multi-axle tracking control [32]–[34], but

* Corresponding Author, [1] Equal contribution.

This research is supported by the National Research Foundation, Singapore, under its Medium-Sized Center for Advanced Robotics Technology Innovation (CARTIN).

All authors are with the School of Electrical and Electronic Engineering, Nanyang Technological University, 50 Nanyang Avenue, Singapore 639798

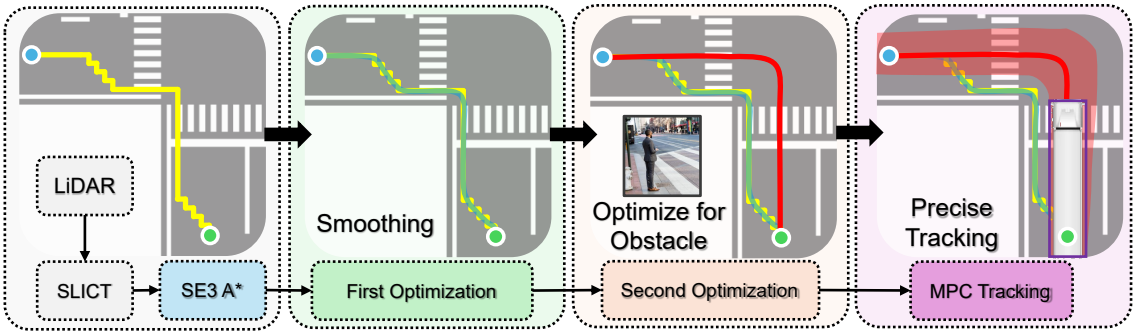

Fig. 2: Overall pipeline: initial path generation, MINCO-based two-stage optimization, and MPC tracking for multi-axle independent steering.

rarely optimize both in one loop. Classical steering structures (Ackermann/AFRS/FWS) restrict instantaneous steering centers and reduce maneuverability for long-wheelbase vehicles [35], [36]. Our method bridges this gap by coupling SDF-based swept-area planning with MPC tracking for independently steerable wheel groups.

In planning, geometric collision checks (e.g., broad-phase + narrow-phase) are efficient but may degrade in cluttered scenes, while SDF-based formulations provide smoother gradients for optimization and better compatibility with continuous trajectories [4], [31]. However, many existing methods optimize only obstacle distance and smoothness, without directly penalizing off-tracking-induced swept area for multi-axle bodies.

In tracking, hierarchical or simplified kinematic models can achieve stable motion [32], yet they usually optimize chassis-level states and defer wheel-level behavior to heuristic mappings. For long vehicles with independent steering groups, this often causes unnecessary lateral envelope growth in turning maneuvers. We therefore keep a compact MPC state model but explicitly map the optimized control to each wheel group, preserving both computational efficiency and geometric consistency.

III. Proposed Solution

A. Problem Statement

Let ξ denote the vehicle top-view shape and h its constant height. Over trajectory $\mathcal{L}(t)$, swept volume is $\mathbb{V} = \cup_{t\in[t_s,t_e]}\xi\mathcal{L}(t)h$; with fixed h, minimizing $\mathbb{V}$ is equivalent to minimizing swept area $\mathbb{S}$. We optimize trajectory control points $\{(x_j, y_j, \varphi_j) \in \mathbb{SE}(2)\}$ and track them with MPC input $u = [V_x, V_y, \omega]^\top$.

B. Trajectory Planning

The planner has two optimization stages. Starting from an A*-based initial trajectory, we fit a MINCO trajectory and solve

$$\min_{q,T} \ \mathbb{W}_E J_E + \mathbb{W}_T J_T + \mathbb{W}_P J_P \tag{1}$$

to obtain a smooth trajectory close to the seed path. We then refine it by adding obstacle and swept-area terms:

$$\min_{q,T} \ \mathbb{W}_E J_E + \mathbb{W}_T J_T + \mathbb{W}_{ob} J_{ob} + \mathbb{W}_{sv} J_{sv}. \tag{2}$$

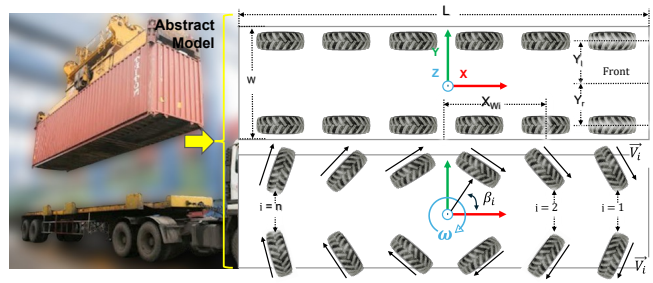

Fig. 3: Vehicle parametric model used for SDF-based obstacle/swept-area costs.

Here, J_{ob} is computed from a rectangular-vehicle SDF in map coordinates [4], and

$$J_{sv} = \sum_j \left(\varphi_j - \arctan\frac{V_{Y,j}}{V_{X,j}}\right)^2 \tag{3}$$

penalizes misalignment between vehicle heading and path tangent to reduce swept area. LBFGS and LMBM are used for the two stages, respectively [37], [38]. For swept-area SDF evaluation, we parallelize map-point minimum-distance search with CUDA.

For a vehicle-frame point $P_{veh} = [X_{veh}, Y_{veh}]^T$, the rectangular SDF is built from

$$dx = |X_{veh}| - \frac{L}{2}, \qquad dy = |Y_{veh}| - \frac{W}{2}, \tag{4}$$

and

$$f_{SDF}(P_{veh}) = \begin{cases} \sqrt{dx^2 + dy^2}, & dx > 0,\ dy > 0, \\ \max(dx, dy), & \text{otherwise}. \end{cases} \tag{5}$$

For completeness, the path-deviation term in the first stage is

$$J_P = \sum_{j=1}^{N-1} \|P_j - P_{A^*,j}\|_2^2, \tag{6}$$

which keeps the trajectory close to the feasible A* seed while allowing smoothing. In the second stage, obstacle cost is accumulated over sampled obstacles and trajectory points using the vehicle-frame SDF with safety threshold d_{th}. This yields gradients suitable for quasi-Newton updates and improves optimization stability in narrow passages.

The practical effect of J_{sv} is to align the vehicle longitudinal axis with local path tangents. This reduces corner swing and tail overhang during left/right turns, which is critical for multi-axle vehicles near curbs or pedestrians. The two-stage strategy also improves convergence: stage 1 provides a smooth initialization, and stage 2 focuses on safety and swept-area reduction.

1) Swept Area Estimation: Given trajectory pose $(R(t), T(t))$, the SDF of map point P to the vehicle body at time t is

$$F_{\text{SDF}}(P,t) = f_{\text{SDF}}\left(R^{-1}(t)(P - T(t))\right). \tag{7}$$

Swept-area SDF uses the minimum value along the trajectory horizon,

$$f^*_{\text{SDF}}(P) = \min_{t\in[t_{min},t_{max}]} F_{\text{SDF}}(P,t). \tag{8}$$

We solve the inner minimization with Armijo line search [39]. On an $\mathbb{N}\times\mathbb{N}$ map grid, CUDA parallelization evaluates all points simultaneously, enabling real-time swept-area updates.

C. Trajectory Tracking

The tracking model uses state $\mathbf{X} = [x, y, \varphi]^T$ and control $u = [V_x, V_y, \omega]^T$:

$$\mathbf{X}(k+1) = A\mathbf{X}(k) + Bu(k), \tag{9}$$

$$Y = \Psi\mathbf{X}(k) + \Theta U. \tag{10}$$

The MPC objective is

$$\begin{aligned} &\min_U J = \frac{1}{2}U^T HU + g^T U, \\ &\text{s.t.} \begin{cases} U_{\min} \le U \le U_{\max} \\ \Delta U_{\min} \le \Delta U \le \Delta U_{\max} \end{cases} \end{aligned} \tag{11}$$

After solving the QP, $u_{\text{best}} = [V_x, V_y, \omega]^T$ is converted to wheel-group commands. For wheel group i at (X_{wi}, Y_{wi}):

The prediction and control horizons are denoted by N_p and N_c, respectively. We stack future states into Y and control inputs into U, and use quadratic weights to balance tracking error and control effort. Increment constraints on ΔU suppress aggressive command changes, which improves stability when the vehicle transitions from straight motion to high-curvature turning. The stacked variables are

$$Y = \begin{bmatrix} \mathbf{X}(k+1) \\ \vdots \\ \mathbf{X}(k+N_p) \end{bmatrix}, \quad U = \begin{bmatrix} u(k) \\ \vdots \\ u(k+N_c-1) \end{bmatrix},$$

and

$$J = (Y - Y_t)^T Q_Q (Y - Y_t) + U^T R_R U, \tag{12}$$

which is transformed into

$$\min_U \ \frac{1}{2}U^T HU + g^T U, \tag{13}$$

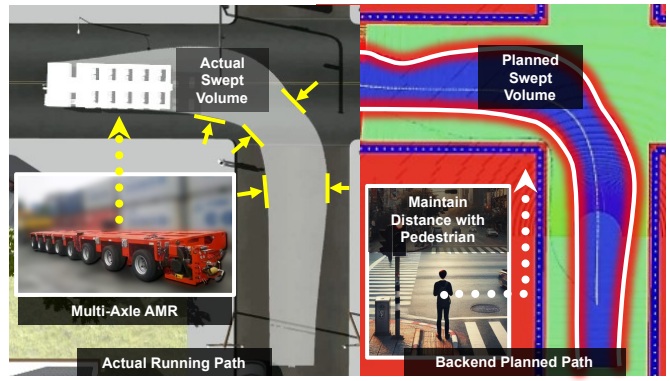

Fig. 4: Simulation scenario and trajectory tracking result in Gazebo.

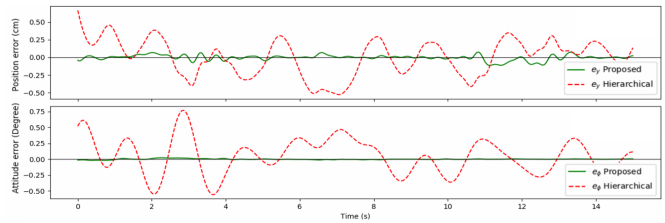

Fig. 5: Tracking error comparison across methods.

$$H = \Theta^T Q_Q \Theta + R_R, \tag{14}$$

$$g = \Theta^T Q_Q (\Psi\mathbf{X}(k) - Y_t). \tag{15}$$

The input increment is constrained by

$$\Delta U = E_{N_c}^{-1}(U - U_{k-1}), \tag{16}$$

with bounds $\Delta U_{min} \le \Delta U \le \Delta U_{max}$.

The wheel velocity is

$$\vec{V_i} = \begin{bmatrix} V_{ix} \\ V_{iy} \end{bmatrix} = \begin{bmatrix} V_x + V_{\tau ix} \\ V_y + V_{\tau iy} \end{bmatrix} = \begin{bmatrix} 1 & 0 & Y_{wi} \\ 0 & 1 & X_{wi} \end{bmatrix} \begin{bmatrix} V_x \\ V_y \\ \omega \end{bmatrix}. \tag{17}$$

Therefore, the final steering angles γ_i and the linear speed V_i of each wheel group are expressed as follows:

$$\gamma_i = \arctan\left(\frac{V_{iy}}{V_{ix}}\right), \tag{18}$$

$$V_i = \sqrt{(V_{ix})^2 + (V_{iy})^2}. \tag{19}$$

This maps MPC outputs to steering angle γ_i and speed V_i for each wheel group.

IV. Experiment

A. System Setup

This work is designed for multi-axle swerve-drive AMRs in future logistics. However, due to hardware limitations, we rely on simulations to verify performance. As shown in Fig. 4, a street map is set up in Gazebo, where a pedestrian is standing at a crosswalk, preparing to cross the road. A 5-axle Swerve-Drive Vehicle, approximately 8.1m long and 2.7m wide, equipped with a LiDAR sensor in front, is making

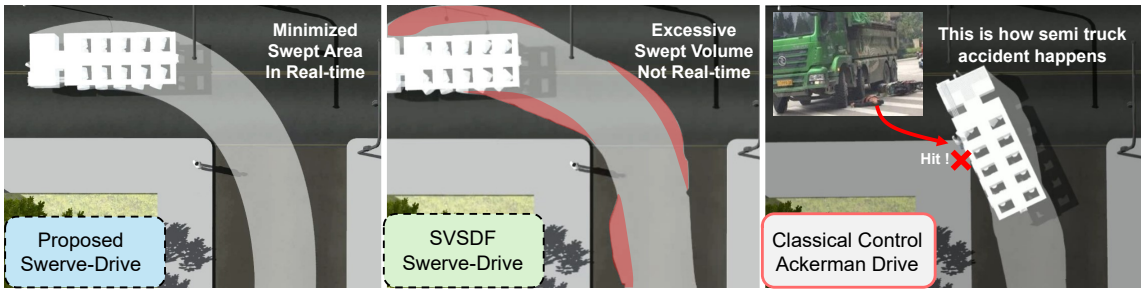

Fig. 6: Qualitative comparison of swept-area envelopes. The proposed method keeps the smallest occupied region in turning.

TABLE I: Comparison of Metrics for Different Methods

Method	$\mathbb{S}_{\text{excess}}$ (m^2)	t (s)	e_y (m)	e_φ $(°)$
Classic [1]	82.15	1.50	±1.38	±3.6
SVSDF [5]	75.62	2.5	±0.04	±0.04
Hierarchical [32]	48.37	1.38	±0.13	±0.12
Proposed	**23.14**	**1.17**	**±0.04**	**±0.03**

Classic [1] and Hierarchical [32] are designed solely for tracking the trajectory generated by our proposed multi-axle AMR planner. SVSDF [5] only has planning, and control is done using our proposed MPC .

a left turn at the intersection. The objective is to plan a path that minimizes the $\mathbb{S}$ while keeping the Swept area away from obstacles to ensure pedestrian safety. The path is tracked using an MPC controller. All the experiments are done on a Gen 13 i7 Notebook PC with Nvidia 4060 GPU.

B. Evaluation Metric

The evaluation metric for our work is listed as follows:

- **Excess Swept Area $\mathbb{S}_{\text{excess}}$:** The additional volume covered by the vehicle beyond the minimal swept area, defined as the difference between the actual and minimal swept area, as illustrated in Fig. 1.
- **Planning Time t:** Quick trajectory generation is vital for real-time applications.
- **Tracking Error e_y, e_φ:** Accurate tracking ensures safe and efficient path execution.

C. Result and Discussion

Table I and **Fig. 5** present a comparison of various methods based on selected evaluation metrics. The Classic method refers to the trajectory tracking approach proposed by [1], where we set the model to allow only the front wheels to steer, simulating a traditional truck. The Hierarchical method is based on the trajectory tracking approach from [32]. The SVSDF method corresponds to the trajectory planning approach from [5], and it is designed to use our MPC controller to track the generated trajectory. Both the Classic and Hierarchical methods are designed solely for tracking the trajectory generated by our proposed multi-axle AMR planner. For the Hierarchical and SVSDF methods, we use a Multi-Axle Swerve-Drive AMR model, where all-wheel groups are steerable.

The proposed method achieves the smallest $\mathbb{S}_{\text{excess}}$, measuring 23.14 m^2, which is the minimal excessive swept area by the vehicle. This is crucial for avoiding obstacles and ensuring pedestrian safety. Although the Classic and Hierarchical methods track the trajectory generated by our proposed approach, their poor tracking performance results in a significantly larger $\mathbb{S}_{\text{excess}}$ making them much less effective compared to our method. In terms of trajectory planning time, our method significantly outperforms others, with a reduced planning time of 1.17 seconds. The Classic and Hierarchical methods are designed to use the trajectory generated by our proposed approach, which results in similarly fast trajectory generation times. This improvement is critical for real-time applications where rapid responses to environmental changes are required.

For trajectory tracking performance, our approach maintains the lateral tracking error, e_y, within ±0.04 m and the heading angle error, e_φ, within ±0.03°. Compared to the Hierarchical method, our approach demonstrates substantial improvements in both precision and reliability, thereby enhancing the safety and maneuverability of the vehicle. Since the SVSDF method is designed to use our proposed tracking method, it achieves similar accuracy in tracking error performance.

We conducted a comparative analysis with different AMR models, as shown in Fig. 6. The proposed methods achieve minimal swept areas and accurate trajectory tracking without collisions, providing significant improvements for modern AMRs. While SVSDF reduces collision risk, its swept volume is still suboptimal. The classical truck control method performed the worst, with the largest swept area and frequent collisions, as commonly reported in industrial settings and news sources. This highlights the effectiveness of our approach in minimizing swept volume and enhancing safety.

V. Conclusion

This paper presented a unified approach combining swept volume-aware path planning with MPC to optimize trajectories and independently control each wheel of multi-axle AMRs for precise maneuvering in constrained environments. By calculating wheel group steering angles from velocity vectors, we simplify the vehicle model and enhance MPC control. Simulations show reduced swept volume and improved real-time trajectory tracking using CUDA, supporting reliable and efficient autonomous heavy-duty AMR applications.

REFERENCES

[1] H. Zhao, Z. Liu, Z. Li, S. Zhou, W. Chen, C. Suo, and Y.-H. Liu, "Modelling and dynamic tracking control of industrial vehicles with tractor-trailer structure," in *2019 IEEE/RSJ International Conference on Intelligent Robots and Systems (IROS)*. IEEE, 2019.

[2] F. Islam, A. Vemula, S.-K. Kim, A. Dornbush, O. Salzman, and M. Likhachev, "Planning, learning and reasoning framework for robot truck unloading," in *2020 IEEE International Conference on Robotics and Automation (ICRA)*. IEEE, 2020, pp. 5011–5017.

[3] S. Yuan, H. Wang, and L. Xie, "Survey on localization systems and algorithms for unmanned systems," *Unmanned Systems*, vol. 9, no. 02, pp. 129–163, 2021.

[4] T. Zhang, J. Wang, C. Xu, A. Gao, and F. Gao, "Continuous implicit sdf based any-shape robot trajectory optimization," in *2023 IEEE/RSJ International Conference on Intelligent Robots and Systems (IROS)*. IEEE, 2023, pp. 282–289.

[5] J. Wang, T. Zhang, Q. Zhang, C. Zeng, J. Yu, C. Xu, L. Xu, and F. Gao, "Implicit swept volume sdf: Enabling continuous collision-free trajectory generation for arbitrary shapes," *ACM Transactions on Graphics (TOG)*, vol. 43, no. 4, pp. 1–14, 2024.

[6] X. Liu, A. K. Madhusudhanan, and D. Cebon, "Experimental evaluation of minimum swept-path control for autonomous reversing of articulated vehicles," in *2020 IEEE Intelligent Vehicles Symposium (IV)*. IEEE, 2020, pp. 584–589.

[7] Y. Yang, D. Chen, T. Qin, X. Mu, C. Xu, and M. Yang, "E2e parking: Autonomous parking by the end-to-end neural network on the carla simulator," in *2024 IEEE Intelligent Vehicles Symposium (IV)*. IEEE, 2024, pp. 2375–2382.

[8] R. Bai, R. Zheng, M. Liu, and S. Zhang, "Multi-robot task planning under individual and collaborative temporal logic specifications," in *2021 IEEE/RSJ International Conference on Intelligent Robots and Systems (IROS)*. IEEE, 2021, pp. 6382–6389.

[9] J. Bian, J. Zhang, K. Guo, W. Li, X. Yu, and L. Guo, "Risk-aware path planning using cvar for quadrotors," in *2023 6th International Symposium on Autonomous Systems (ISAS)*. IEEE, 2023, pp. 1–6.

[10] R. Jin, Y. Gao, Y. Wang, Y. Wu, H. Lu, C. Xu, and F. Gao, "Gs-planner: A gaussian-splatting-based planning framework for active high-fidelity reconstruction," in *2024 IEEE/RSJ International Conference on Intelligent Robots and Systems (IROS)*. IEEE, 2024, pp. 11 202–11 209.

[11] S. Liu, K. Guo, X. Yu, L. Ma, L. Xie, and L. Guo, "Safe maneuvering planning for flights in complex environments," *IEEE Transactions on Industrial Electronics*, vol. 71, no. 5, pp. 4944–4953, 2023.

[12] M. Cao, K. Cao, S. Yuan, K. Liu, Y. L. Wong, and L. Xie, "Path planning for multiple tethered robots using topological braids," in *Robotics: Science and Systems*, 2023.

[13] M. Cao, K. Cao, S. Yuan, T.-M. Nguyen, and L. Xie, "Neptune: non-entangling trajectory planning for multiple tethered unmanned vehicles," *IEEE Transactions on Robotics*, vol. 39, no. 4, pp. 2786–2804, 2023.

[14] Q. Li and S. Yuan, "Jacquard v2: Refining datasets using the human in the loop data correction method," in *2024 IEEE International Conference on Robotics and Automation (ICRA)*, 2024, pp. 7932–7938.

[15] C. Zhao, E. Wang, K. Guo, and X. Yu, "Design and anti-disturbance control for an h-configuration tiltable quadrotor: Enabling narrow space crossing," *IEEE Transactions on Aerospace and Electronic Systems*, 2024.

[16] Z. Yang, J. Jia, Y. Liu, K. Guo, X. Yu, and L. Guo, "Trace: Trajectory refinement with control error enables safe and accurate maneuvers," in *2024 IEEE 18th International Conference on Control & Automation (ICCA)*. IEEE, 2024, pp. 154–161.

[17] D. Fan, Q. Liu, C. Zhao, K. Guo, Z. Yang, X. Yu, and L. Guo, "Flying in narrow spaces: Prioritizing safety with disturbance-aware control," *IEEE Robotics and Automation Letters*, 2024.

[18] H. Yu, C. Hu, J. Wang, G. Lu, J. Tu, Z. Zheng, J. Li, and F. Gao, "Aggressive collision-inclusive motion planning," *IEEE/ASME Transactions on Mechatronics*, 2024.

[19] R. Bai, S. Yuan, K. Li, H. Guo, W.-Y. Yau, and L. Xie, "Realm: Real-time line-of-sight maintenance in multi-robot navigation with unknown obstacles," in *IEEE International Conference on Robotics and Automation (ICRA)*, 2025.

[20] K. Cao, D. Li, and L. Xie, "Bearing-ratio-of-distance rigidity theory with application to directly similar formation control," *Automatica*, vol. 109, p. 108540, 2019.

[21] F. Liu, S. Yuan, W. Meng, R. Su, and L. Xie, "Non-cooperative stochastic target encirclement by anti-synchronization control via range-only measurement," in *2023 IEEE International Conference on Robotics and Automation (ICRA)*. IEEE, 2023, pp. 5480–5485.

[22] Z. Hu, X. Li, and M. Meng, "A stackelberg game approach for three-player autonomous racing," in *2023 42nd Chinese Control Conference (CCC)*. IEEE, 2023, pp. 4886–4891.

[23] M. Cao, Y. Lyu, S. Yuan, and L. Xie, "Online trajectory correction and tracking for facade inspection using autonomous uav," in *2020 IEEE 16th International Conference on Control & Automation (ICCA)*. IEEE, 2020, pp. 1149–1154.

[24] F. Liu, S. Yuan, W. Meng, R. Su, and L. Xie, "Multiple noncooperative targets encirclement by relative distance-based positioning and neural antisynchronization control," *IEEE Transactions on Industrial Electronics*, vol. 71, no. 2, pp. 1675–1685, 2023.

[25] X. Xu, M. Cao, S. Yuan, T. H. Nguyen, T.-M. Nguyen, and L. Xie, "A cost-effective cooperative exploration and inspection strategy for heterogeneous aerial system," in *Proceedings of the 2024 IEEE International Conference on Control and Automation (ICCA)*. IEEE, 2024.

[26] M. J. Er, S. Yuan, and N. Wang, "Development control and navigation of octocopter," in *2013 10th IEEE International Conference on Control and Automation (ICCA)*. IEEE, 2013, pp. 1639–1643.

[27] J. Jia, W. Zhang, K. Guo, J. Wang, X. Yu, Y. Shi, and L. Guo, "Evolver: Online learning and prediction of disturbances for robot control," *IEEE Transactions on Robotics*, 2023.

[28] F. Liu, S. Yuan, K. Cao, W. Meng, and L. Xie, "Distance-based multiple noncooperative ground target encirclement for complex environments," *IEEE Transactions on Control Systems Technology*, vol. 33, no. 1, pp. 261–273, 2025.

[29] M. Ji, K. Pan, X. Zhang, Q. Pan, X. Dai, and Y. Lyu, "Integration of sense and control for uncertain systems based on delayed feedback active inference," *Entropy*, vol. 26, no. 11, p. 990, 2024.

[30] H. Lee, J. Park, C. Koo, J.-C. Kim, and Y. Eun, "Cyclops: Open platform for scale truck platooning," in *2022 International Conference on Robotics and Automation (ICRA)*. IEEE, 2022, pp. 8971–8977.

[31] H. Wang, Y. Lin, W. Zhang, W. Ye, M. Zhang, and X. Dong, "Safe autonomous exploration and adaptive path planning strategy using signed distance field," *IEEE Access*, vol. 11, 2023.

[32] F.-x. Xu, C. Zhou, and X.-h. Liu, "Hierarchical control strategies for multi-mode steering system of emergency rescue vehicle," *Mechatronics*, vol. 85, p. 102834, 2022.

[33] W. Wang, J. Li, X. Li, Z. Li, and N. Guo, "Multi-objective collaborative control method for multi-axle distributed vehicle assisted driving," *Applied Sciences*, vol. 13, no. 13, p. 7769, 2023.

[34] Z. Zhang, X.-j. Ma, C.-g. Liu, and S.-g. Wei, "Dual-steering mode based on direct yaw moment control for multi-wheel hub motor driven vehicles: Theoretical design and experimental assessment," *Defence Technology*, vol. 18, no. 1, pp. 49–61, 2022.

[35] S. Chaudhuri, V. Saini, and M. Singh, "Kinematic analysis of multi-axle steering system for articulated vehicle," SAE Technical Paper, Tech. Rep., 2009.

[36] Y. Ye, L. He, and Q. Zhang, "Steering control strategies for a four-wheel-independent-steering bin managing robot," *IFAC-PapersOnLine*, vol. 49, no. 16, pp. 39–44, 2016.

[37] A. Coppola and B. M. Stewart, "lbfgs: Efficient l-bfgs and owl-qn optimization in r," 2020.

[38] N. Karmitsa, "Limited memory bundle method and its variations for large-scale nonsmooth optimization," *Numerical Nonsmooth Optimization: State of the Art Algorithms*, pp. 167–199, 2020.

[39] L. Armijo, "Minimization of functions having lipschitz continuous first partial derivatives," *Pacific Journal of mathematics*, vol. 16, no. 1, pp. 1–3, 1966.